Article

Potential Applications of Low Altitude Remote Sensing for Monitoring Jellyfish

Young-Heon Jo*†, Hongsheng Bi and Jongsuk Lee***

*Department of Oceanography, Pusan National University, Busan, 609-735, Republic of Korea
**Chesapeake Biological Laboratory, University of Maryland Center for Environmental Science, Solomons, MD 20688, USA

Abstract : Jellyfish (cnidarian) are conspicuous in many marine ecosystems when in bloom. Despite their importance for the ecosystem structure and function, very few sampling programs are dedicated to sample jellyfish because they are patchily distributed and easily clogged plankton net. Although satellite remote sensing is an excellent observing tool for many phenomena in the ocean, their uses for monitoring jellyfish are not possible due to the coarse spatial resolutions. Hence, we developed the low altitude remote sensing platform to detect jellyfish in high resolutions, which allow us to monitor not only horizontal, but also vertical migration of them. Using low altitude remote sensing platform, we measured the jellyfish from the pier at the Chesapeake Biological Laboratory in Chesapeake Bay. The patterns observed included discrete patches, in rows that were aligned with waves that propagated from deeper regions, and aggregation around physical objects. The corresponding areas of exposed jellyfish on the sea surface were 0.1×10^4 pixel^2, 0.3×10^4 pixel^2, and 2.75×10^4 pixel^2, respectively. Thus, the research result suggested that the migration of the jellyfish was related to the physical forcing in the sea surface.

Key Words : low altitude remote sensing, morphology algorithm, jellyfish, sea state

1. Introduction

Gelatinous zooplankton are increasingly recognized as key components that affect ecosystem structure and function (e.g. Malakoff 2001; Daskalov *et al*., 2007; Richardson *et al*., 2009; Condon *et al*., 2011). Although historical evidence is insufficient to reach firm conclusions on the global rise of gelatinous zooplankton (Condon *et al*., 2012; Condon *et al*., 2013), mounting evidence suggests that the structure of pelagic ecosystems can change rapidly from one dominated by fish to a less desirable state dominated by gelatinous zooplankton in response to anthropogenic perturbations like eutrophication and overfishing (Malakoff 2001; Purcell *et al*., 2007; Richardson *et al*., 2009). Jellyfish blooms can have profound impacts on pelagic food webs and they negatively impact commercial and recreational activities. The abundance of gelatinous species tends to be highly variable in both space and time, yet remarkably little is known about

the factors that control this variability. Many cnidarian jellyfish reproduce rapidly via strobilation from abundant benthic polyps giving rise to high population densities, but this does not explain the extreme patchiness that is typically observed.

In Chesapeake Bay, the sea nettle (*Chrysaora quinquecirrha* (Desor, 1848)) often become seasonally abundant (> 20 m-3) in mesohaline waters during the summer due to temperature-cued strobilation in the late spring (Decker *et al*., 2007), but their abundances often showed large spatial and intra- and inter- annual variation. Matanoski and Hood (2006) showed that the swimming behavior of these organisms contributes to this variability. Coherent swarms of sea nettles have been observed at relatively small scales (1-5 meters), which may be related to either foraging or reproductive behaviors. Vertical migration may allow these organisms to take advantage of oppositely flowing currents at the surface and bottom of the estuary to maintain position in optimal habitat, which may affect distributions at a range of scales (Haury *et al*., 1978). Many species of zooplankton have been shown to use vertical swimming behaviors to control their position in estuaries (reviewed in Naylor, 2006).

The fluctuations in jellyfish abundance are often affected by environmental conditions, particularly temperature and salinity or the climatic patterns that affect them (reviewed by Purcell 2005; and see also Lynam *et al*., 2005; Brodeur *et al*., 1999). Studies in the Chesapeake Bay have explored the environmental factors that influence the distribution and abundance of *C*. *quinquecirrha* medusae with the goal of explaining and predicting the location and intensity of the summer bloom (e.g., Cargo and King, 1990; Decker *et al*., 2007). The Decker *et al*. (2007) habitat model predicts the probability of *C*. *quinquecirrha* occurrence in Chesapeake Bay by assessing salinity and temperature conditions that are most favorable for sea nettles. This model corresponds well to observations of the seasonal cycle of sea nettle abundance, but does not explain the differences in abundance between different tributaries.

Recent advances in optical and acoustic sampling technologies have made it possible to characterize spatial variability in gelatinous zooplankton populations over a wide range of scales, even in the turbid waters of Chesapeake Bay. Here we developed low altitude airborne remote sensing to characterize the spatial variability in sea nettle populations (and their prey) over scales ranging from a few meters to tens of kilometers. Based on the observations, we analyzed horizontal and vertical migrations of the jellyfish. Accordingly, this study is arranged by introducing a new observing system and an algorithm to determine the edge of the jellyfish in the water in Section 2, illustrating our analysis for jellyfish behaviors in Section 3, and concluding our results in Section 4.

2. Observation System and Methods

Low Altitude Remote Sensing System: A low altitude monitoring system uses various sensors and a Helikite (Helium balloon + Kite) to obtain continuous imagery with very high spatial resolution. This system has many advantages over other remote sensing observation systems (aerial and satellite remote sensing, unmanned aerial vehicle and blimp) because it can be used on demand at much lower cost, with much shorter lead time, and almost no influences of weather (the system flies below clouds, is waterproof and withstands wind speeds up to 18 m/sec) for up to 1 month without recharging the helium gas (Fig. 1). As Fig. 1 shows, the imagery can be obtained at fixed location and/or along a towed path by a boat, so that one can monitor specific sites as long as needed at a fixed location or survey large areas by making mosaics of the imagery.

The system consists four components: helikite, sensors, tether and winch. The helikite is for holding the sensors in the air as long as needed. The sensors are the most important parts to collect sea surface
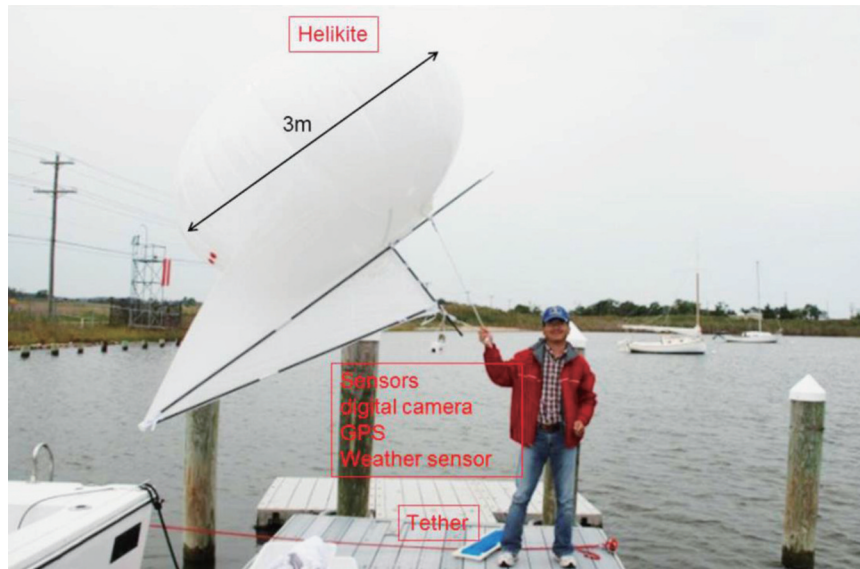
Fig. 1. Low altitude remote sensing system. Sensors include a video and digital camera, weather sensor, and transmitter.

informations remotely. For this study we used a digital camera, but many other optical sensors can be used and synclonized with Inertial Motion Unit (IMU) for correcting imagery in terms of georeferencing. Tether is another important component for holding the helikite so that the winds cannot take away the system. The winch is almost necessary to operate the low altitude remote sensing system. If the wind is strong when one tries to pull it back to the ground, it is not easy to do that because of the strong tensing on the tether by the winds. Thus, the power windch is really useful to dragging it down. For the specific applications for the low altitude remote sensing platform, Jo *et al*.(2015) employed the similar system to map waterlines based on concecutive imageries. The study illustrated that the system can provide high spatial resolutions of the water depths through different stateges of the waterlines.

This system can obtain images in various spatial resolutions (1cm to 80cm) from multiple altitudes (100m to 2km) simultaneously. At lower altitude and very high spatial resolution the system generates a smaller map (50m×50m), and at higher altitude and moderate spatial resolution the system generates a larger map (2km×2km) at the same time. In addition to the remote sensing system, georeferencing images are very important processes to obtain the same spatial resolution in a geo-located map. However, there is no high spatial resolution of map for georeferencing all imagery. Thus, we used a reference image to map all imagery in the same geo-locations, as illustrated in Jo *et al*.(2015, their Fig. 7). Therefore, the low altitude remote sensing system provides another new, complimentary means of characterizing the patchiness and movement of large gelatinous zooplankton that can be used to quantify the horizontal distribution of *C. quinquecirrha* near the surface and also the movement of aggregations, and it can guide in situ subsurface optical and acoustic surveys.

Fig. 2 is an example for deploying this system. We collected over 100 images with a 1cm spatial resolution every 10 second near the Chesapeake Biological Laboratory, Solomons, Maryland, USA. One can see the fish and jellyfish as well as the 18 m long pier. The fish and jellyfish appeared in Fig. 2 could be validated visually on the sight when the imagery were taken from Helikite. As we analyzed the jellyfish patches in the many consecutive images, edge detection algorithms are necessary to describe the dynamics and movement
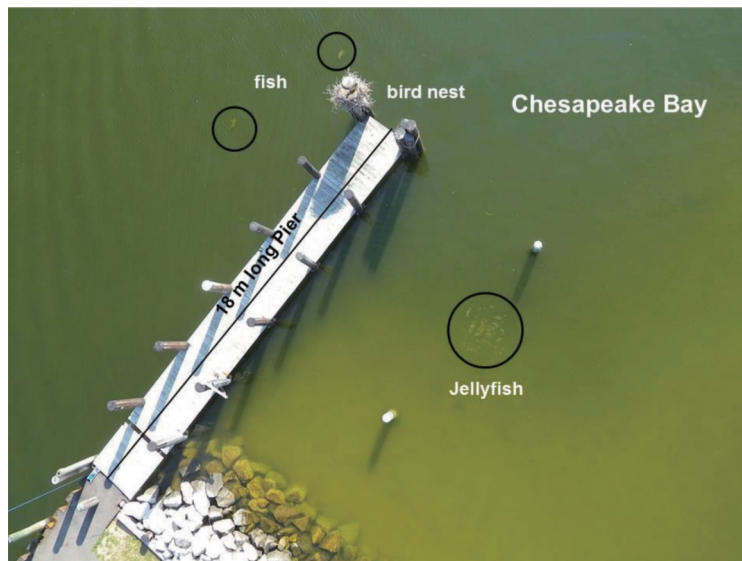
Fig. 2. An example imagery taken by low altitude remote sensing. *C. quinquecirrha* is identified by visual identification from the pier.

of jellyfish patches. The methods are introduced in the following section.

Algorithm for detecting the edge of jellyfish patches: In order to determine the edge of the group of the jellyfish, we used the morphology method including erosion and dilation (Ridler and Calvard, 1978; Chen and Chen, 2009; Gonzalez and Woods, 1992). In order to determine erosion and dilation, threshold is needed to be defined as follows,

$$T_{k+1} = \frac{1}{2} \left(\frac{\sum_{i=0}^{T_k} i \cdot h[i]}{\sum_{i=0}^{T_k} h[i]} + \frac{\sum_{i=T+1}^{255} i \cdot h[i]}{\sum_{i=T+1}^{255} h[i]} \right) \quad (1)$$

$$\mu_1 = \frac{\sum_{i=0}^{T_k} i \cdot h[i]}{\sum_{i=0}^{T_k} h[i]}, \mu_1 = \frac{\sum_{i=T+1}^{255} i \cdot h[i]}{\sum_{i=T+1}^{255} h[i]} \quad (2)$$

Where, T is an initial threshold. Iterate processing that divides pixels into A group of $T >$ gray level and B group of $T <$ gray level until find out an appropriate threshold. Calculate a threshold value of $(k + 1)$th repetitively. When $T_{k+1} = T_k$, T_{k+1} is defined as a final threshold value.

Specifically, morphology method includes erosion that serves to remove the noise and reduce the size of the object and dilation that serves to fill the empty space inside the object and increase the size of the object.

$$A \ominus B = \{z \mid (B)_z \cap A^c = \emptyset\}$$
$$A \ominus B = \{z \mid (\hat{B})_z \cap A = \emptyset\} \quad (3)$$

Where, A is the structuring element, and B is the objectives in the image. $A \ominus B$ is the erosion of A by B. $A \oplus B$ is the dilation of A by B. In order to determine right edge detection as defined with Equation 3, many iterations will be conducted to determine the threshold as shown with Equation 2.

The morphology algorithm was employed to determine the edge of the jellyfish patches, which were used to estimate the areas of them and center of the jellyfish patches.

Center of jellyfish patches: To determine the center of the jellyfish patches, we used the following equations.

$$x = \frac{\sum x_i}{n} \text{ and } x = \frac{\sum y_i}{n} \quad (4)$$

Where, x_i and y_i are the points of the x and y-positions covered by the jellyfish patches. Thus, x and y represent

the center of the jellyfish patches.

3. Results

1) Detecting jellyfish

Although many studies reported how much jellyfish is important in the ecosystem, there are no direct observations. The abundances of jellyfish can be estimated by observations. As Fig. 2 shows, the low altitude remote sensing system can observe many objects in high resolutions. One can see the fishes, a bird nest and aggregated jellyfish. From the many different features of the *C. quinquecirrha*, we categorized three different *C. quinquecirrha* (species identification confirmed visually from the pier) aggregations in response to sea surface state. The patterns observed included discrete patches (Fig. 3a) and in rows that were aligned with waves that propagate from deeper regions (Fig. 3b), and aggregation around physical objects (Fig. 3c).

Then, a following question is that how we can determine the edge of the jellyfish patches? Fig. 4a is the jellyfish patch that taken from Fig. 2. Figs. 4b to 4c are the grayscale conversion, after threshold processing, and morphological image processing for jellyfish area,

respectively. It is very clear that the white parts in Fig. 4d are the objective jellyfish patch from Fig. 4a. It is worth to note that we can observe not only groups of jellyfish, but also individual ones due to high spatial resolutions. Fig. 5 is the magnified image for the individual jellyfish. Figs. 5b to 5f show the gray scale conversion (5b), background extraction for removing a non-uniformed background (5c), after threshold processing (5d), morphological image processing (combining dilation and erosion) (5e) and the final result for jellyfish area (5f), respectively. Accordingly, the final results can be used to estimate the exposed areas on the sea surface that is discussed in next Section.

2) Horizontal and vertical migration of jellyfish

Swimming behavior is important in determining sea nettle population distributions in Chesapeake Bay over a wide range of time and space scales and that this contributes substantially to the observed variability. Images in the same area were collected and processed to map aggregation trajectories (Fig. 6). Large images can be used to map the spatial distribution of *C. quinquecirrha* near the surface and small images can be used to monitor the movement of patches as shown with Figs. 3a-d. As Fig. 6 shows, the jellyfish migrates
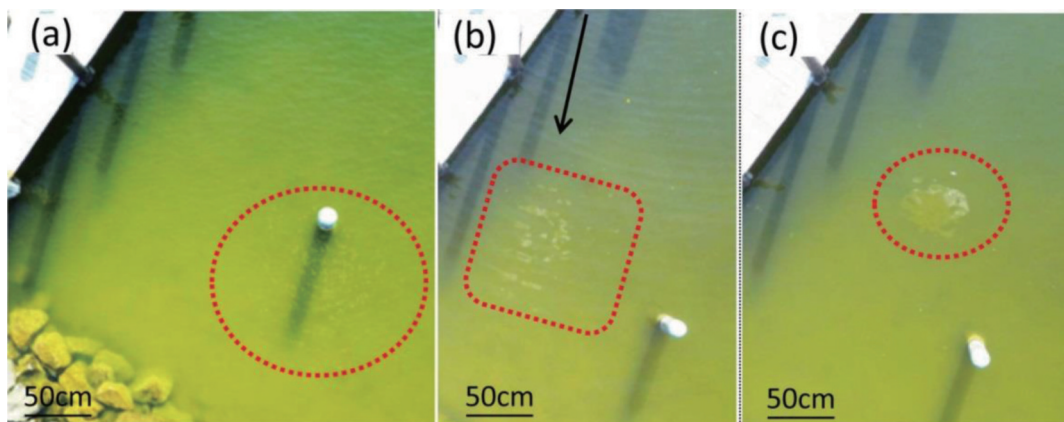

Fig. 3. Three examples of observed aggregation patterns are those grouped around white pole (a) aligned with waves (b) and grouped (c) taken in Chesapeake Bay.
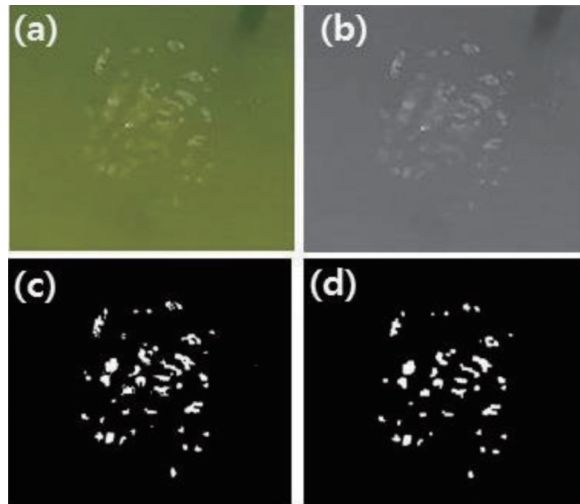
Fig. 4 The jellyfish patch observed in Chesapeake Bay using low altitude remote sensing. Jellyfish patch taken from Fig. 2 (a), grayscale conversion (b), after threshold processing (c), and morphological image processing (combining dilation and erosion) (d).
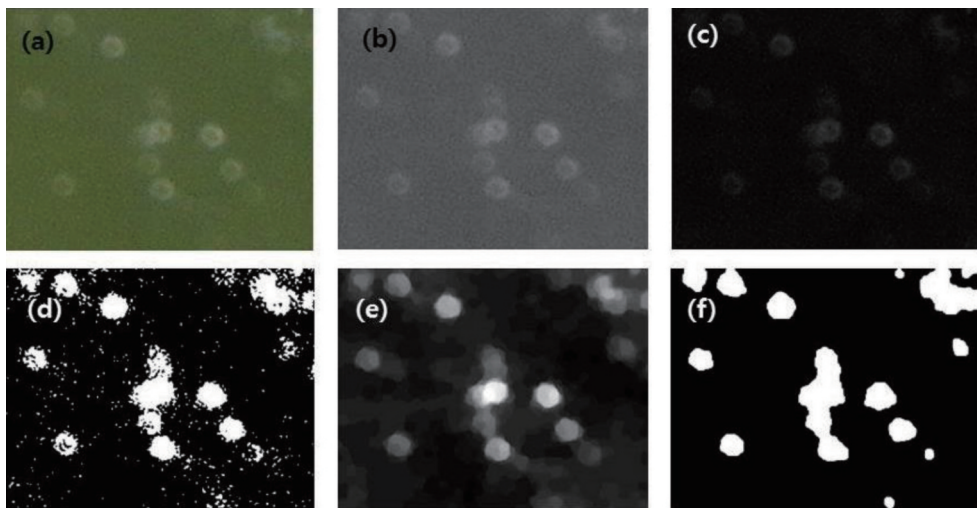

Fig. 5. Magnified individual *C. quinquecirrha*. Original image (a) that taken from Fig. 3a, grayscale conversion (b), background extraction for removing a non-uniformed background (c), after threshold processing (d), morphological image processing (combining dilation and erosion) (e), and the final result for jellyfish area (f).

as a group around the white wood pole. The center of the locations (Equation 4) are indicated with numbers from 1 to 45. The location 1 is shown with the jellyfish features as an example (Fig. 2). Other locations of the jellyfish were processes as the same manner, as illustrated in Fig. 4. Although we do not know exactly what makes them move, the potential reason is the different physical sea state, as discussed with Fig. 3. In addition, the exposed areas of the jellyfish were specific

estimated.

The areas of the exposed on the sea surface were estimated based on the algorithm as illustrated in Fig. 4. Fig. 7 shows the time series of the exposed areas of the jellyfish. The lower area on 230 seconds shown with the first green circle corresponds to the scattered features (0.1×10^4 pixel^2), as shown in Fig. 3a. The second green circle on 310 seconds is due to the aligned with waves. At this stage the jellyfish aggregated along
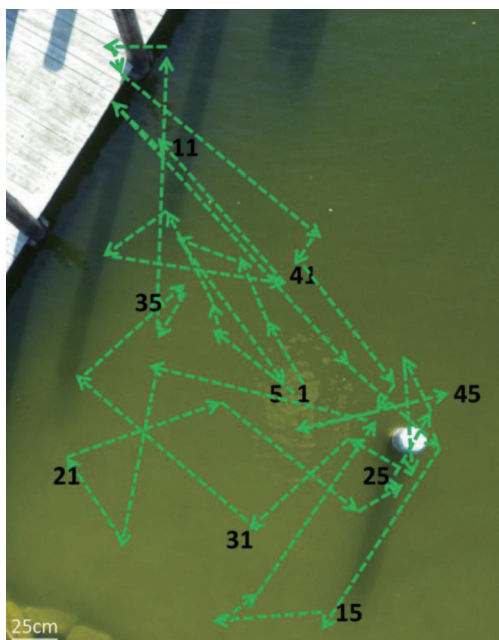
Fig. 6. The trajectory of a *C. quinquecirrha* aggregation based on the centroid of the patch. The gray color represents the jellyfish observed at 7:40:44AM (Shown with "1"). The location of aggregation was recorded every 10 seconds for 450 seconds.

jellyfish suggest that we can understand how the jellyfish migrate in response to the different sea state. The rougher the sea surface is the deeper the jellyfish migrates.

4. Conclusion

Through the development of the novel new observations of sea nettle population variability in Chesapeake Bay, the low altitude remote sensing will enhance our ability to understand the food web, commercial, and recreational impacts of this organism, and potentially provide an improved understanding of the behavioral and hydrodynamic factors that control gelatinous zooplankton populations globally. Using low altitude remote sensing system, we successfully observe the jellyfish movements continuously. Then, the jellyfish patches in the consecutively imagery were objectively mapped based on the morphology algorithm. Accordingly, our findings are as follows.

1. The system could map not only jellyfish patches as a group, but also the individuals after magnifying the images.

2. The different behavior of the jellyfish depends on the different sea state: scattered, aggregated and

with waves so that the exposed regions of groups are relatively larger (0.3×10^4 pixel²), as shown in Fig. 3b. The third green circle at the time of 390 seconds (2.75×10^4 pixel²) occurs when jellyfish aggregated so that the exposed regions are the largest, as shown in Fig. 3c. This time series of exposed surface areas of
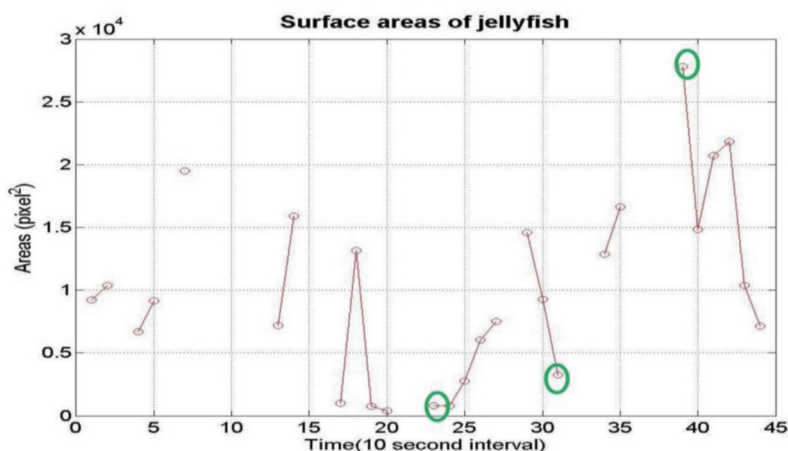

Fig. 7. Exposed areas of jellyfish patches. The three green circles indicated the areas when the three different groups shown in Fig. 3. When jellyfish migrated to the under pier, jellyfish areas were not estimated so that there are missing points.

aligned with waves.

3. While the scattered features are due the relatively rough sea surface, the aggregated features are due to the calm sea state. In addition, the aligned to the wave is due to the travelling waves there.

4. We also could observe that jellyfish migrates to under the pier nearby and swim around the pole. The reason of the migration may need a hydrodynamic model to simulate the different physical conditions to examine their behaviors.

5. The exposed areas of the jellyfish on the sea surface suggest that the jellyfish vertically migrates in response to the sea surface state. As denoted earlier, the jellyfish avoid the strong rough sea state so that they migrate to the deeper layer.

It is worth to note that there are some uncertainties in the Helikite image processes because an altimeter and IMU were not installed on the Helikite in this experiment. For the spatial resolution, we could estimate spatial resolutions of 14 mega pixels camera from a $50m \pm 2m$ altitude, which corresponds to $10cm \pm 0.4cm$ per pixel. For the geo-location, we used the fishing pier and the while pole. When we selected these Ground Control Points (GCP), there might be 2pixel errors, which is 20cm of uncertainties. For projection, we estimated the angles of four distorted corners when we employed the geo-referencing processes (not shown), resulting from the changing camera viewing angles by the winds. Thus, the georeferenced image (not shown) show the actually adjusted imagery with distorted angles. Since the viewing angle changes from nadir to less than 10 degrees, uncertainties due to the image projection is about 0.7cm.

In order to improve the current low altitude remote sensing system, two additional components has to be added for better image processes: the IMU and Ground Control Points (GCP) for synchronizing all imagery for correct geo-referencing. These two components will allow us to determine right geo-referencing and projection. For the future works, we can use a combination of in situ imaging and acoustic measurements combined with low altitude remote sensing to characterize the 3-D distributions and patchiness of *C. quinquecirrha* (and their prey). Then, these data can be used in combination with coupled 3-D hydrodynamic-biogeochemical-behavioral models to determine how both physical and biological factors influence *C. quinquecirrha* abundance and distribution over a wide range of spatial scales in Chesapeake Bay. Improving our ability to predict when and where high concentrations of these organisms are likely to occur is therefore important for understanding both the food web and human impacts of *C. quinquecirrha*.

Acknowledgement

References

Brodeur, R.D., C.E. Mills, J.E. Overland, G.E. Walters, and J.D. Schumacher, 1999. Evidence for a substantial increase in gelatinous zooplankton in the Bering Sea, with possible links to climate change, *Fisheries Oceanography*, 8(4): 296-306.

Cargo, D.G., and D.R. King, 1990. Forecasting the Abundance of the Sea Nettle, Chrysaora quinquecirrha, in the Chesapeake Bay, *Estuaries and Coasts*, 13(4): 486-491.

Chen, Y.B. and O.T.C. Chen, 2009. Image Segmentation Method Using Thresholds Automatically Determined from Picture Contents, *EURASIP Journal on Image and*

Video Processing, 2009(1): 140492.

Condon, R.H., D.K. Steinberg, P.A. Del Giorgio, T.C. Bouvier, D.A. Bronk, W.M. Graham, and H.W. Ducklow, 2011. Jellyfish blooms result in a major microbial respiratory sink of carbon in marine systems. *Proc. of the National Academy of Sciences*, 108(25): 10225-10230.

Condon, R.H., W.M. Graham, C.M. Duarte, K.A. Pitt, C.H. Lucas, S.H.D. Haddock, K.L. Robinson, M.N. Dawson, M.B. Decker, C.E. Mills, J.E. Purcell, A. Malej, H. Mianzan, S. Uye, S. Gelcich, and L.P. Madin, 2012. Questioning the rise of gelatinous zooplankton in the world's oceans. *BioScience*, 62(2): 160-169.

Condon, R.H., C.M. Duarte, K.A. Pitt, K.L. Robinson, C.H. Lucas, K.R. Sutherland, H.W. Mianzan, M. Bogeberg, J.E. Purcell, M.B. Decker, S. Uye, L.P. Madin, R.D. Brodeur, S.H.D. Haddock, A. Malej, G.D. Parry, E. Eriksen, J. Quiñonesr, M. Achah, M. Harveys, J.M. Arthurd, and?W.M. Grahamt, 2013. Recurrent jellyfish blooms are a consequence of global oscillations, *Proc. of the National Academy of Sciences*, 110(3): 1000-1005.

Cowan, J.H., and E.D. Houde, 1993. Relative predation potentials of scyphomedusae, ctenophores and planktivorous fish on ichthyoplankton in Chesapeake Bay, *Marine Ecology-Progress Series*, 95: 55-65.

Daskalov, G.M., A.N. Grishin, S. Rodionov, and V. Mihneva, 2007. Trophic cascades triggered by overfishing reveal possible mechanisms of ecosystem regime shifts, *Proc. of the National Academy of Sciences*, 104(25): 10518-10523.

Decker, M.B., C.W. Brown, R.R. Hood, J.E. Purcell, T.F. Gross, J.C. Matanoski, R.O. Bannon, and E.M. Setzler-Hamilton, 2007. Predicting the distribution of the scyphomedusa Chrysaora quinquecirrha in Chesapeake Bay, *Marine Ecology Progress Series*, 329: 99-113.

Feigenbaum, D., and M. Kelly, 1984. Changes in the lower chesapeake bay food-chain in presence of the sea nettle Chrysaora quinquecirrha (Scyphomedusa), *Marine Ecology Progress Series*, 19: 39-47.

Gonzalez, R. and R. Woods, 1992. *Digital Image Processing*, Addison-Wesley Publishing Company.

Haury, L.R., J.A. Mcgowan, and P.H. Wiebe, 1978. Patterns and processes in the time-space scales of plankton distributions, *Spatial pattern in plankton communities*. Springer US.

Jo, Y.H., J. Sha, J.I. Kwon, K. Jun, and J. Park, 2015. Mapping bathymetry based on waterlines observed from low altitude Helikite remote sensing platform, *Acta Oceanologica Sinica*, 34(9): 110-116.

Kimmel, D.G., W.R. Boynton, and M.R. Roman, 2012. Long-term decline in the calanoid copepod Acartia tonsa in central Chesapeake Bay, USA: An indirect effect of eutrophication?, *Estuarine, Coastal and Shelf Science*, 101: 76-85.

Lynam, C.P., S.J. Hay, and A.S. Brierley, 2005. Jellyfish abundance and climatic variation: contrasting responses in oceanographically distinct regions of the North Sea, and possible implications for fisheries, *Journal of the Marine Biological Association of the United Kingdom*, 85(03): 435-450.

Naylor, E., 2006. Orientation and navigation in coastal and estuarine zooplankton, *Marine and Freshwater Behaviour and Physiology*, 39(1): 13-24.

Malakoff, D., 2001. Interest blooms in growing jellyfish boom, *Science*, 293(5527): 29.

Matanoski, J.C., and R.R. Hood, 2006. An individual-based numerical model of medusa swimming behavior, *Marine Biology*, 149(3): 595-608.

Purcell, J.E., 1992. Effects of predation by the scyphomedusan Chrysaora quinquecirrha on

zooplankton populations in Chesapeake Bay, USA, *Marine Ecology-Progress Series*, 87: 65-76.

Purcell, J. E., 1997. Pelagic cnidarians and ctenophores as predators: selective predation, feeding rates, and effects on prey populations, I*n Annales de l'Institut océanographique*, 73(2): 125-137.

Purcell, J.E., and J.H. Cowan, 1995. Predation by the scyphomedusan Chrysaora quinquecirrha on Mnemiopsis leidyi ctenophores, *Marine Ecology Progress Series*, 129: 63-70.

Purcell, J.E., F.P. Cresswell, D.G. Cargo, and V.S. Kennedy, 1991. Differential ingestion and digestion of bivalve larvae by the scyphozoan Chrysaora quinquecirrha and the ctenophore Mnemiopsis leidyi, *The Biological Bulletin*, 180(1): 103-111.

Purcell, J.E., and M.B. Decker, 2005. Effects of climate on relative predation by scyphomedusae and ctenophores on copepods in Chesapeake Bay during 1987-2000, *Limnology and Oceanography*, 50(1): 376-387.

Purcell, J.E., D.A. Nemazie, S.E. Dorsey, E.D. Houde, and J.C. Gamble, 1994. Predation mortality of bay anchovy Anchoa mitchilli eggs and larvae due to scyphomedusae and ctenophores in Chesapeake Bay, *Marine Ecology Progress Series*, 114: 47-58.

Purcell, J.E., S. Uye, and W.T. Lo, 2007. Anthropogenic causes of jellyfish blooms and their direct consequences for humans: a review, *Marine Ecology Progress Series*, 350: 153-174.

Richardson, A.J., A. Bakun, G.C. Hays, and M.J. Gibbons, 2009. The jellyfish joyride: causes, consequences and management responses to a more gelatinous future, *Trends in ecology & evolution*, 24(6): 312-322.

Ridler, T.W. and S. Calvard, 1978. Picture thresholding using an iterative selection method, IEEE *Transactions on Systems, Man, and Cybernetics*, 8(8): 630-632.